

# Dynamic channel blocker/equalizer with high blocking extinction ratio

**Shuping Wang**, MEMBER SPIE  
University of North Texas  
College of Engineering  
3940 North Elm Street  
Denton, Texas 76207  
E-mail: shuping@unt.edu

**Chi-Hao Cheng**, MEMBER SPIE  
Miami University  
School of Engineering and Applied Science  
Oxford, Ohio 45056

**Yanqing Lu**  
Nanjing University  
National Laboratory of Solid State  
Microstructures  
Nanjing, China

**Charles Wong**  
RadiSys Company  
5445 Northeast Dawson Creek Drive  
Hillsboro, Oregon 97124

**Abstract.** The effect of an interpixel gap on light leakage in a free-space liquid-crystal-based dynamic channel blocker/equalizer is studied. The electric field components along the driving electric field within the liquid crystal interpixel gap are numerically calculated. The results show non-uniform distributions in both width and thickness. The numeric results on the relation between gap width and electric field distribution are also presented. A 20-channel, 200-GHz channel-spacing blocker/equalizer on the C band with flat tops and a 40-dB extinction ratio is fabricated and examined.

© 2008 Society of Photo-Optical Instrumentation Engineers. [DOI: 10.1117/1.2841045]

Subject terms: channel blocker; wavelength equalizer; optical filter.

Paper 070400R received May 11, 2007; revised manuscript received Aug. 30, 2007; accepted for publication Sep. 17, 2007; published online Feb. 25, 2008.

## 1 Introduction

The dynamic channel blocker/equalizer (DCBE) is a fundamental building block for reconfigurable optical add/drop multiplexer (ROADM) and optical crossconnect (OXC) nodes within a dense wavelength division multiplexing (DWDM) network. Individual channels (wavelengths) of optical traffic are dynamically routed in a timely manner within this network. The DCBE allows individual wavelengths in the DWDM fiber to be passed, blocked, or equalized dynamically in routing nodes controlled electronically. A number of technical approaches for the use of the ROADM and/or OXC have been explored, including arrayed waveguide gratings (AWGs),<sup>1</sup> fiber Bragg gratings (FBGs),<sup>2</sup> and free-space optical systems.<sup>3-5</sup> Of these, free-space configurations are attractive because of their easy upgradeability, cost effectiveness, and large channel handling capability. Microelectromechanical systems (MEMS)<sup>3</sup> and liquid crystal (LC)<sup>4,5</sup> are two major technologies investigated widely in the free-space configuration of the DCBE. The key advantages of using LC instead of MEMS include no moving parts and proven reliability. Figure 1 depicts the schematic of a two-port DCBE. The multiwavelength light ( $\lambda_1$  to  $\lambda_8$ ) in the DWDM fiber is coupled into the DCBE input. Depending on the amount of the electric voltage applied to the wavelength manipulating units (LC cells in the LC approach), the individual wavelengths can be passed,

attenuated, or blocked. Channels 3, 5, and 6 are blocked, and the remaining channels are equalized, as shown in Fig. 1.

A key technical issue for the OADM and OXC designs is reducing cross talk, which can severely degrade system performance. In fact, the interference caused by the leakage of signal into adjacent channels can be a main source of errors and the major limit of the network size. To avoid the interference between the remainder of the blocked signal and the signal added to the same wavelength in ROADM or OXC, a DCBE with a high extinction ratio and low inter-channel leakage is necessary. In other words, a seamless concatenation of adjacent cells for continuous filtering characters requires a carefully designed LC array (i.e., LC cells and the interpixel gaps). If the interpixel gap is too small, the voltage applied to one cell may affect the adjacent cell by extending its fringe field into the adjacent LC cell. On the other hand, if the interpixel gap is too large, the light may leak through the interpixel gap when both channels are supposed to be blocked. However, to the best of our knowledge, no study focusing on interpixel gap leakage has been conducted. Clearly, to optimize the DCBE's driv-

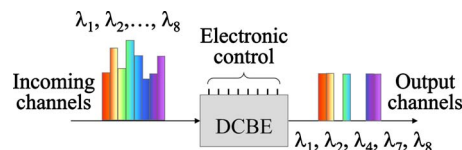
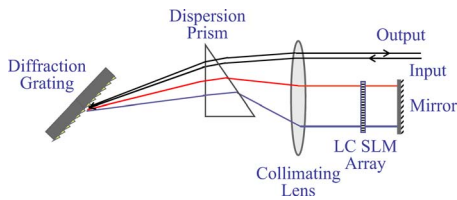


Fig. 1 Schematic of a DCBE.



**Fig. 2** The concept of a free-space DCBE consisting of a linear array of LC SLMs combined with a diffraction grating.

ing voltage and provide appropriate predictions for the device's performance, we must thoroughly study the driving electrical field distributions, especially those within the interpixel gap of the LC cells, before any realistic design can be possible. In this work, we present both simulation and experimental studies of a C-band 20-channel 200-GHz channel-spacing LC-based DCBE with a 40-dB extinction ratio.

## 2 Liquid-Crystal-Based Free-Space Dynamic Channel Blocker/Equalizer

Figure 2 depicts the concept of a free-space DCBE that consists of a linear array of LC spatial light modulators (SLMs) combined with a diffraction grating. The input multiwavelength light impinges on the diffraction grating surface, where the light is angularly diffracted in space as a function of the wavelength. The diffracted light passes through the LC SLM array that controls the individual wavelengths to be passed, blocked, or equalized by applying different amounts of the electric voltage to the LC cells. A mirror is used to fold the optical path back, making the device more compact. The wavelengths reflected by the mirror pass through the SLMs a second time, allowing a more effective modulation. A dispersion prism is added to compensate for the nonlinear wavelength distribution of the diffraction grating. The collimating lens is used to collimate the input light and focus the refracted light to the mirror plane. Because diffraction efficiency is dependent on polarization, the beam displacer (BD) and the half-wave plate (not shown in the figure) are used to convert the input light entering the diffraction grating into a single-polarization light to achieve high efficiency and reduce polarization-dependent loss.

As mentioned before, the manipulation of the individual channels is implemented by an array of LC SLMs in which individual cells are controlled by the driving voltage. The LC SLM array is formed by the twisted nematic LC sandwiched between two parallel glass plates coated with indium tin oxide (ITO). One plate, with ITO fully covered, is used as the common electrode for the driving electronics. The LC SLMs are defined by the patterned ITO cells on the other plate. The thickness of the LC is chosen by design to produce a  $\lambda/2$  retardance. To illustrate the "passed" and the "blocked" states, Fig. 3 depicts the side view of the combination of one LC SLM and the mirror. The LC SLM consists of an LC cell placed between two BDs. The input light with random polarization is split by the first BD into two orthogonally polarized components, namely the ordinary ray (represented by the dots in the figure) and the extraordinary ray (represented by the bars in the figure). If the input light into the DCBE needs to be passed, a zero

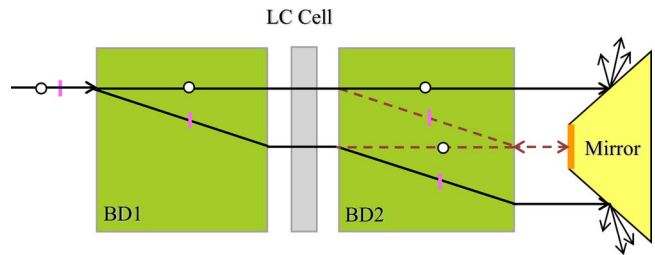


**Fig. 3** Side view of the combined LC SLM and mirror.

voltage is applied to the LC cell. When two orthogonally polarized components pass through it, the LC rotates the polarization states by 90 deg; therefore, the two components are recombined when they leave the second BD and fall normal to the mirror. The light paths within the second beamsplitter in the "passed" state are represented as dash lines in Fig. 3. The mirror reflects the light back to its original path. On the other hand, if the light needs to be blocked, a "blocked state" voltage is applied to the LC cell, so that the polarization states of the two orthogonally polarized components to the LC cell remain unaffected. Hence, they are scattered after leaving the second BD and subsequently hit the coarse side walls of the mirror block. In other words, in the blocked state, LC birefringence is removed by applied voltage. As shown in the next section, in the blocked state, any remaining LC birefringence can decrease the DCBE extinction ratio. The light paths within the second beamsplitter in the blocked state are represented as solid lines in Fig. 3.

Special attention is needed when several sequential channels in the DCBE are driven to the blocked state. If the electric fields in the interpixel gap region are not strong enough to align the molecules in the direction of the driving electric field, the birefringence that causes the light leakage will be seen in this region. We developed a mathematical model to simulate the electrical field distribution in LC cells. The simulation program allows driving electrodes, with various patterns, to be placed in different positions. It uses a "nodal analysis" method to model the LC array. The LC array is divided into  $k \times k$  grids. For each node, Kirchhoff's current law is applied. By solving a linear equation set, the program finds voltages at each node, and then elec-

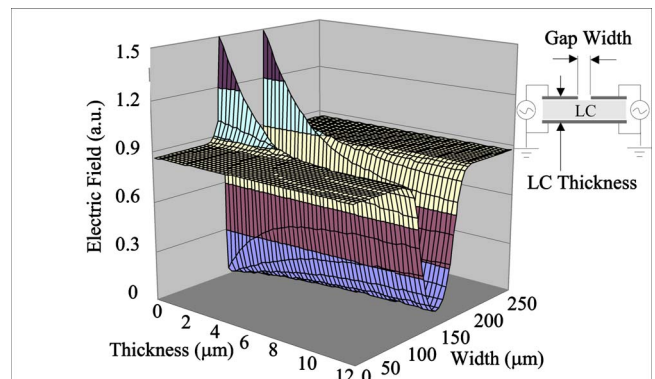


**Fig. 4** Electric field underneath the ITO electrodes and between the LC cells.

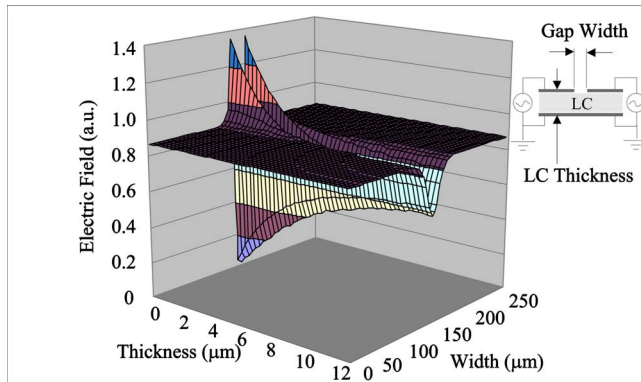


**Fig. 5** Electric field underneath the ITO electrodes and between the LC cells.

tric field distributions are calculated. The simulation model is not only applicable to dc electrical field but also valid for ac signals. For ac driving signals, each grid should be considered as a parallel connection of a resistor and a capacitor. The voltage applied across each grid will be determined by the relative impedance of the grid. The simulation of the electric field distribution across the interpixel gap allows us to estimate the LC gap effect on DCBE performance. Figure 4 illustrates the simulation results of the electric field underneath the ITO electrodes and between the LC cells (one gap and part of two adjacent electrodes are shown, though 20 channels are simulated). The electric field shown in the simulation results denotes the field components along the driving electric field, which affect the LC molecules' alignment. The voltage applied to the LC is 5 V. The gap width between the electrodes, which are 200  $\mu\text{m}$  wide, is 50  $\mu\text{m}$ . The thickness of the LC cell is 11  $\mu\text{m}$ . The data show that the electric fields in the gap area are small and reach the minimums in the middle of the gap with only 10% or less of that underneath the ITO electrodes. The simulation suggests that when two adjacent channels are driven to the blocked states, the LC molecules between the electrodes do not align perfectly to the driving electric field, because of the weak and nonuniform field in this region, resulting in birefringence that prevents the light from being completely blocked. The sharp electric field peaks shown in Fig. 4 (and in Fig. 5 later) are due to the edge effect of the ITO electrodes.

The situation is improved when the interpixel gap width is reduced, and the pixel pitch remains at 250  $\mu\text{m}$ . Figure 5 depicts the electric field distribution underneath the ITO electrodes and between the LC cells. The gap width is 12  $\mu\text{m}$  (i.e., 238- $\mu\text{m}$  ITO width), and the rest of the parameters remain the same. As expected, the electric field reaches the minimum in the middle of the interpixel gaps; however, along the thickness direction, toward the ground electrode, the minimum field strength gradually increases and eventually attains approximately 70% of the strength underneath the electrodes.

The interactive effect between LC cells for different gap sizes is studied. The maximum acceptable gap width that guarantees no light leakage through the interpixel gaps when adjacent channels are supposed to be blocked is chosen based on the simulation combined with the single LC

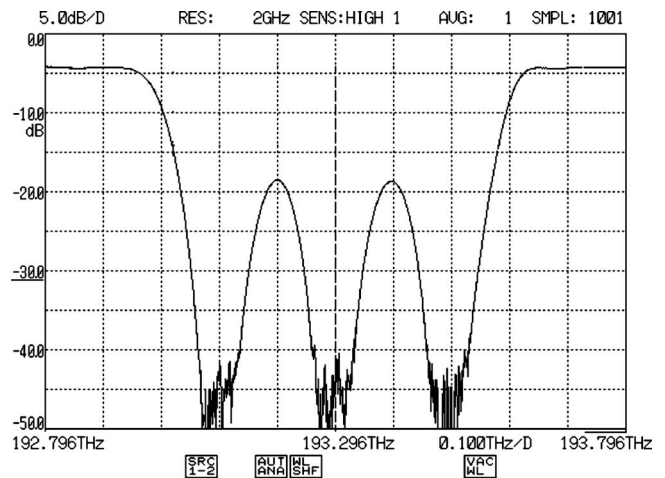


**Fig. 6** Experimental results of the output spectrum with three adjacent channels blocked for a DCBE with a 50- $\mu\text{m}$  interpixel gap.

cell experiment. With fixed channel spacing, the “optimal” gap width can be determined based on the specifications on the passband bandwidth, blockband bandwidth, isolation, etc. In other words, DCBE specifications behave as the constraint as we try to determine the “optimal” interpixel gap width of LC array. Other factors, such as the type of LC and how the driving voltage is applied, affect gap width selection. In our study, a 10- $\mu\text{m}$  gap width is determined, as described in the following section, to be the optimal interpixel gap width that gives the desired bandwidths.

### 3 Experimental Results

A free-space 20-channel 200-GHz channel-spacing DCBE on the C band (1531.116 to 1561.419 nm) is fabricated with emphasis on the study of the interpixel gap effect on light leakage. An 1100-line/mm diffraction grating with a physical dimension of  $9.5 \times 7 \times 4$  mm is used. The thickness of the LC, 11  $\mu\text{m}$ , is controlled by the spacers placed between two glass plates with ITO electrodes that define the LC cells. The LC cells repeat every 250  $\mu\text{m}$  with interpixel gaps of 50  $\mu\text{m}$  (i.e., 200- $\mu\text{m}$  ITO electrode width).

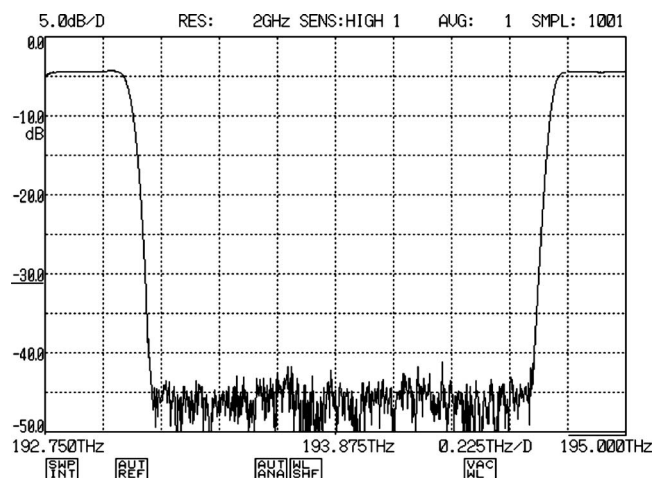


**Fig. 7** Transmitted power as a function of frequency when seven adjacent channels are blocked. The interpixel gap width is 10  $\mu\text{m}$ .

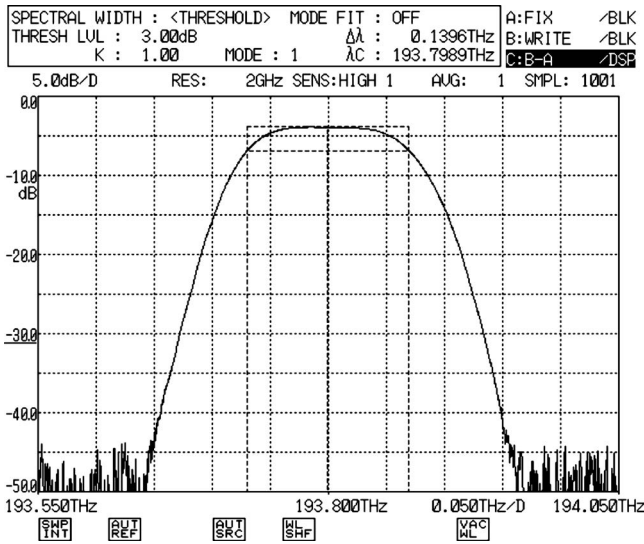


**Fig. 8** The 3-dB bandwidth for a passed channel measured to be 140 GHz.

Figure 6 depicts the experimental result of the output power as a function of frequency for the device. The figure shows three blocked adjacent channels. The device has an insertion loss (IL) of less than 5 dB for the passed channels, and an extinction ratio of about 40 dB at the center of the blocked channels. Power leakages with a peak value of approximately 18 dB through the interpixel gaps are observed, which are not unexpected. Based on the simulation results presented in Sec. 2, the electrical field within the gap becomes smaller and reaches its minimums (nearly zero) at the center of the gap. The reduced field strength and the field's nonuniformity in the gap region prevent the LC molecules from rotating their polarization to the blocked state, thus yielding the maximum light leakage at the center of the interpixel gaps.

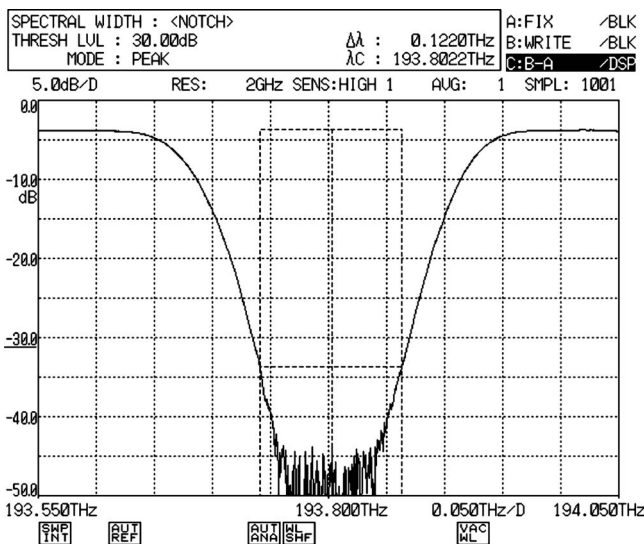


**Fig. 9** The 30-dB bandwidth for a blocked channel measured to be 122 GHz.

**Table 1** Bandwidths from the peak IL for blocked channels.

IL (dB)	30	25	15	10
Block channel bandwidth (GHz)	122	140	178	203

To improve the light leakage caused by the interpixel gap effect, a 200-GHz channel-spacing DCBE with a reduced gap width of 10  $\mu\text{m}$  (i.e., 240- $\mu\text{m}$  ITO electrode width), which is otherwise identical to the first DCBE, is fabricated. Based on the simulation results, when the gap width is decreased, the strength of the electric field within the gap region is increased. The field strength in the middle of the gap reaches 80% or more underneath the ITO electrodes in the region close to the ground electrode. With the fold-back design of the DCBE, the light passes the LC SLMs twice; therefore, the modulation is enhanced. Figure 7 depicts transmitted power as a function of frequency when seven adjacent channels are blocked. As expected, a 40-dB extinction ratio is observed, and there are no power leakages through the interpixel gaps. Passed channels have flat tops, and the insertion losses are less than 5 dB.

Figures 8 and 9 depict typical bandwidths for both passed and blocked channels. The 3-dB bandwidth for passed channels is measured to be 140 GHz, as shown in Fig. 8, and the 30-dB bandwidth for blocked channels is 122 GHz, as shown in Fig. 9. More measured bandwidths from the peak IL for both blocked and passed channels are summarized in Tables 1 and 2, respectively.

#### 4 Summary

A free-space 20-channel 200-GHz channel-spacing DCBE with a 40-dB extinction ratio and less than 4-dB IL is presented. Based on our numerical results, the electric field components along the driving electric field within the interpixel gap are not uniformly distributed in width and thickness. The field strength increases with the reduction of gap width. The nonuniformity of the field may cause the LC molecules in this region not to align perfectly with the driving electric field and result in light leakage. On the other hand, if the interpixel gap is too small, the voltage applied to one cell may affect the adjacent cell by extending its fringe field into the adjacent LC cell. Therefore, a thorough understanding of the driving electric field distribution within the interpixel gaps is necessary for designing a high-performance DCBE. The simulation and experimental results presented in this work demonstrate the validity of our simulation model developed to investigate driving electric field distribution within an interpixel gap.

**Table 2** Bandwidths from the peak IL for passed channels.

IL (dB)	0.5	1	3	15	30
Pass channel bandwidth (GHz)	88	105	140	220	274

## References

1. J. B. D. Soole, R. Pafchek, C. Narayanan, G. Bogert, L. Jampabayana, N. Chand, and J. Yu, "DWDM performance of a packaged reconfigurable optical add-drop multiplexer subsystem supporting modular systems growth," *IEEE Photonics Technol. Lett.* **15**(11), 1600–1602 (2003).
2. A. V. Tran, W. D. Zhon, R. C. Tucker, and R. Lauder, "Optical add-drop multiplexers with low crosstalk," *IEEE Photonics Technol. Lett.* **13**(6), 582–584 (2001).
3. J. Ford and J. Walder, "Dynamic spectral power equalization using micro-opto-mechanics," *IEEE Photonics Technol. Lett.* **10**(10), 1440–1442 (1998).
4. O. Solgaard, F. S. A. Sandejas, and D. M. Bloom, "Deformable grating optical modulator," *Opt. Lett.* **17**(9), 688–690 (1992).
5. C. R. Doerr, R. Pafchek, and L. W. Stulz, "16-band integrated dynamic gain equalization filter with less than 2.8-dB insertion loss," *IEEE Photonics Technol. Lett.* **14**(3), 334–336 (2002).

Biographies and photographs of authors not available.